

# The Absorption Spectra of Krypton and Xenon in the Wavelength Range 330–600 Å

K. Codling\* and R. P. Madden

Institute for Basic Standards, National Bureau of Standards, Washington, D.C. 20234

(September 20, 1971)

A total of 153 krypton resonances in the spectral region 330–500 Å and 253 xenon resonances in the spectral region 375–600 Å are reported. A detailed listing of the resonances is given, with wavelength and line shape information. The analysis of the spectra is very incomplete and will require detailed theoretical calculation to significantly improve it. In Kr, 45 resonances and in Xe, 56 resonances have been grouped into probable Rydberg series, for which classifications are suggested. The resonances are due, in the main, to either the excitation of the inner subshell "s" electron ( $s^2p^6 \rightarrow sp^6np$ ) or to the excitation of two of the outer "p" electrons simultaneously ( $s^2p^6 \rightarrow s^2p^4nln'l'$ ). These highly excited states autoionize, resulting in resonances with window-, asymmetric-, or absorption-type profiles. Where possible, comparisons are made with previous work.

Key words: Autoionization; far ultraviolet; krypton; photoionization; resonances; xenon.

## 1. Introduction

This communication is intended as the final report on the absorption spectra of the noble gases He through Xe, observed in the wavelength range 80–600 Å. Earlier papers have dealt with the discovery and analysis (in some cases tentative) of the structure in the photoionization continua of He[1],<sup>1</sup> Ne[2], and Ar[3]. We present here the spectra of Kr and Xe in the wavelength range 330–600 Å. Two previous publications have described the structure observed between 80 and 200 Å, due to the excitation of a single inner-shell *d* electron[4] and also the simultaneous excitation of an outer-shell *p* and an inner-shell *d* electron[5]. (The excitation of the outer *p* electron had been observed many years before [6].)

In the wavelength range 400–500 Å, Samson [7] observed two distinct resonances in the photoionization continuum of Kr using a many-lined spark discharge as a background source. Subsequently, many more autoionizing states in both Kr and Xe between 380 and 600 Å were reported [8] and recently, highlights of the present, more detailed experimental observations of the Kr and Xe spectra have been published [9]. In an accompanying paper [10], absolute cross-section measurements were made in the region of some of the more prominent resonances.

The following analysis of the Kr and Xe spectra is necessarily far from complete. The breakdown of strict *L-S* coupling, evident throughout the Ar spectrum, is even more pronounced in Kr and Xe. Consequently, considerable theoretical work is re-

quired, of an *ab initio* type, before a reasonable analysis of the Kr and Xe spectra can be made. In the hope of stimulating such calculations on noble gas atoms, we present here final numbers on wavelengths of the resonances observed, along with a rough guide as to the profiles of some of the resonances. The accompanying spectra and densitometer traces together with the published resonance profiles [10] may be helpful in comparing theoretical predictions with the experimental observations, at least for the low-lying levels.

## 2. Experimental Procedure

The spectra shown in figure 1 were taken using a three-meter grazing-incidence spectrograph [11]. The grating of 600 lines per mm and a 0.01 mm spectrograph entrance slit yielded a resolution of 0.06 Å. The source of continuum was provided by the radiation emitted by the NBS-SURF (Synchrotron Ultraviolet Radiation Facility). For this synchrotron the radiated power per unit wavelength peaks at 335 Å. Spectra were photographed from 80–600 Å with a grating blazed at 200 Å. The noble gas filled the spectrograph at pressures typically in the range of 0.01 to 0.10 torr, with absorption path lengths between entrance slit and plate of the order of 1m. Since the synchrotron continuum is free from overlying emission and absorption lines, any features observed were due to the gas itself.

The spectra were photographed on Eastman SWR plates.<sup>2</sup> Wavelength calibration was obtained by super-

\*Present Address: University of Reading, Physics Department, Whiteknights Park, Reading, Berks, England.

<sup>1</sup> Figures in brackets indicate the literature references at the end of this paper.

<sup>2</sup> A commercial material is identified in this paper in order to adequately specify the experimental procedure. Such identification does not imply recommendation or endorsement by the National Bureau of Standards.

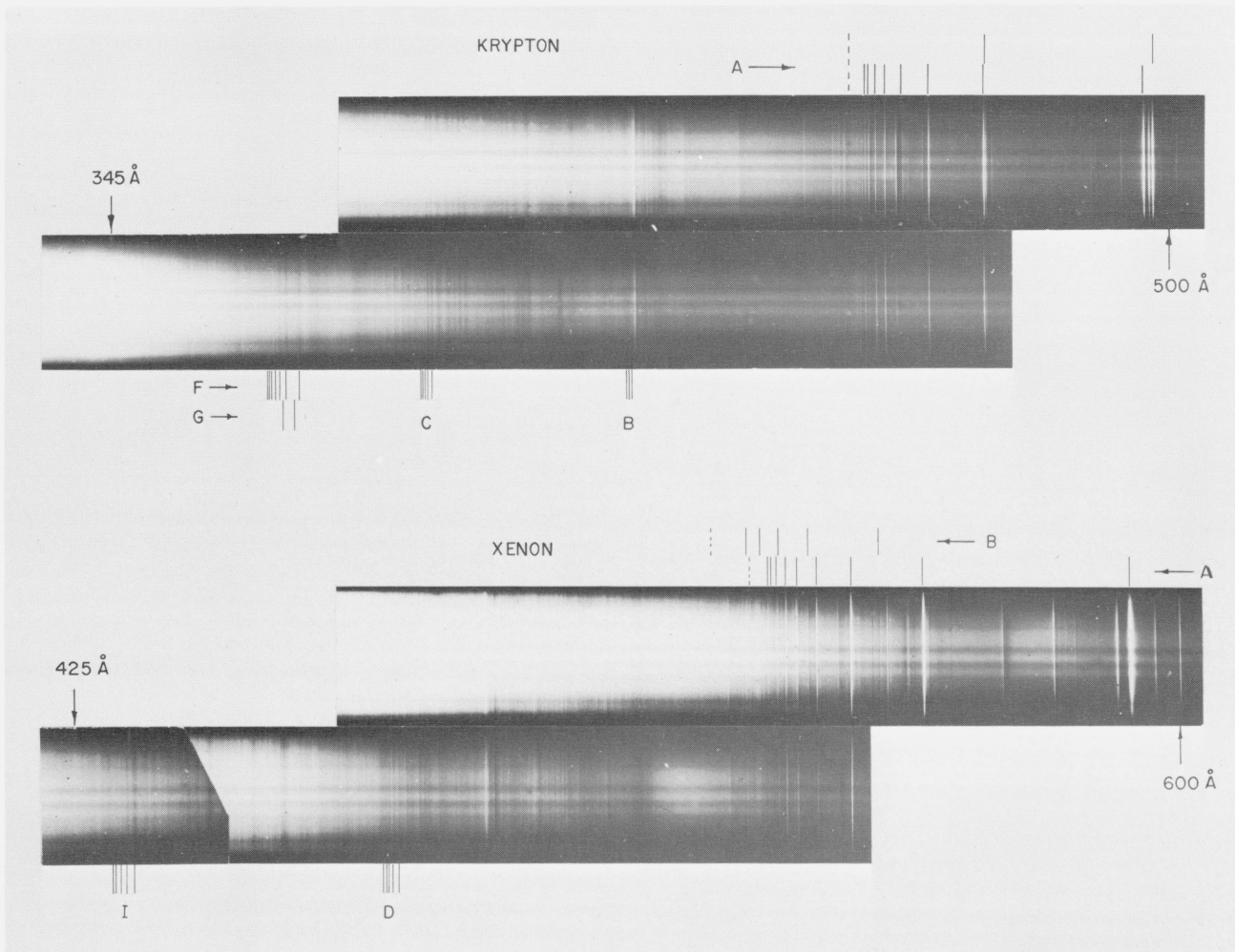


FIGURE 1. *Upper Spectrum.* The absorption spectrum of Kr between 345 and 500 Å, taken at two different pressures to accentuate the various regions of the spectrum.

(The background continuum cross section varies by over a factor of 3 through this region.) Black denotes absorption and therefore the prominent series of resonances due to the excitation of the subshell 4s electron to outer *p* orbitals are of the "window" type. The remaining resonances are due to the simultaneous excitation of two 4*p* electrons. Such resonances, grouped in series B, C, F, and G, are listed in table 3.

*Lower Spectrum.* The absorption spectrum of Xe between 425 and 600 Å, taken at three different pressures.

(The background continuum cross section varies by over a factor of 4 in this region). The prominent series of "window" resonances labeled A, are due to the excitation of a subshell 5s electron to outer *p* orbitals. Short series labeled C, D, and I are due to simultaneous excitation of two 5*p* electrons and are listed in table 4.

imposing the absorption spectrum of He on the Kr and Xe spectra and by using the previously determined fact that wavelengths could be reliably predicted, by application of the grating equation, to an accuracy of at least 0.01 Å. As an additional check, where long Rydberg series existed, use was made of the fact that such series converge in the limit to a well established state of Kr II or Xe II. In the cases where only small perturbations exist good quantum defects were obtained using known limits and the measured wavelengths of the Rydberg series lines.

### 3. Classification of Spectra

The ground state of Kr is  $4s^24p^6\ ^1S_0$ , that of Xe  $5s^25p^6\ ^1S_0$ . The ionization potentials of Kr and Xe are 14.0 and 12.1 eV respectively. Thus, when photons of an energy between 20 and 40 eV are incident upon

these gases, the basic process observed is photoionization. However, as well as exciting an outer *p* electron to continuum  $\epsilon s$  and  $\epsilon d$  states, it is possible to excite a subshell *s* electron to *p*-type orbitals or excite two electrons simultaneously. In the latter case, either two outer *p* electrons or both an outer *p* and a subshell *s* electron can be excited.

Thus, in Kr for example, one may excite to configurations of the type:  $4s4p^6np$  and  $4s^24p^4nl'n'l'$  where  $l'l' = sp, pd, sf, df$ . Transitions of the type  $4s4p^5nl'n'l'$  where  $l'l' = ss, pp, sd$  etc., have not been positively identified in Kr and Xe, although unidentified resonances exist in the appropriate energy region, and the existence of similar excitations has been fairly well established in Ar [3].

The total line list of 153 resonances in Kr and 253 resonances in Xe are listed in terms of their wave-

length, wavenumber and resonance type in tables 1 and 2. By resonance type we mean the following. When a high-lying discrete state such as the  $4s4p^65p$  state of Kr is excited by photoabsorption, the lifetime of this excited state is extremely short ( $\sim 10^{-13}$  s). The state decays into the adjacent continuum by auto-ionization, with the ejection of an energetic electron,

the ion being left in its ground or excited state. The interaction of a discrete state with the continuum of states of similar energy and parity has been dealt with by Fano and Cooper [12]. The resonances in the continuum which result from this interaction may be broad, and can have a variety of profiles.

TABLE 1. Code number, wavelength ( $\lambda$ ), wave number ( $\nu$ ), and profile type for all observed Kr resonances, listed in order of decreasing wavelength

Number	Wavelength ( $\text{\AA}$ )	Wave number ( $\text{cm}^{-1}$ )	Comment <sup>a</sup>	Number	Wavelength ( $\text{\AA}$ )	Wave number ( $\text{cm}^{-1}$ )	Comment <sup>a</sup>
1	<sup>b</sup> 501.23 $\pm$ .05	199509	-sx	52	421.56 $\pm$ .03	237214	-sx
2	498.83 $\pm$ .05	200469	-dw	53	421.23 $\pm$ .03	237400	-sx
3	<sup>c</sup> *497.50 $\pm$ .05	201005	+dw	54	420.90 $\pm$ .05	237586	-sx
4	496.90 $\pm$ .05	201248	dw	55	420.36 $\pm$ .05	237891	-da
5	*496.07 $\pm$ .05	201584	-dw	56	419.96 $\pm$ .05	238118	sa
6	492.52 $\pm$ .05	203037	-sw	57	419.74 $\pm$ .05	238243	sa
7	488.71 $\pm$ .05	204620	-dx	58	419.51 $\pm$ .05	238373	sa
8	488.06 $\pm$ .05	204893	-dx	59	419.10 $\pm$ .10	238607	da
9	472.26 $\pm$ .03	211748	+sw	60	418.83 $\pm$ .03	238760	sw
10	*471.48 $\pm$ .03	212098	+sw	61	418.70 $\pm$ .03	238834	sw
11	*471.23 $\pm$ .03	212211	-sw	62	418.33 $\pm$ .05	239046	sa
12	469.08 $\pm$ .03	213183	-sx	63	*417.96 $\pm$ .03	239257	sa
13	464.70 $\pm$ .10	215193	-sw	64	*417.62 $\pm$ .03	239452	sa
14	*462.71 $\pm$ .03	216118	+sw	65	*417.39 $\pm$ .05	239584	sa
15	461.83 $\pm$ .03	216530	-sx	66	*417.22 $\pm$ .05	239682	sa
16	460.45 $\pm$ .03	217179	sa	67	416.76 $\pm$ .05	239946	sw
17	459.91 $\pm$ .03	217434	-sa	68	416.01 $\pm$ .10	240379	dw
18	*458.69 $\pm$ .03	218012	+sw	69	<sup>d</sup> 414.78 $\pm$ .10	241092	sw
19	457.86 $\pm$ .03	218407	-sw	70	413.58 $\pm$ .10	241791	sw
20	457.51 $\pm$ .03	218574	sa	71	412.79 $\pm$ .05	242254	+sw
21	456.67 $\pm$ .03	218976	sa	72	412.47 $\pm$ .05	242442	sw
22	*456.12 $\pm$ .03	219241	sw	73	409.70 $\pm$ .2	244081	dda
23	455.29 $\pm$ .03	219640	-sx	74	406.85 $\pm$ .10	245791	da
24	*454.73 $\pm$ .03	219911	sw	75	405.30 $\pm$ .10	246731	da
25	454.01 $\pm$ .03	220259	sa	76	403.34 $\pm$ .05	247930	da
26	*453.73 $\pm$ .03	220395	sw	77	401.50 $\pm$ .2	249070	dda
27	*453.15 $\pm$ .03	220677	sw	78	400.33 $\pm$ .07	249794	da
28	*452.68 $\pm$ .03	220907	sw	79	399.75 $\pm$ .07	250156	da
29	*452.34 $\pm$ .03	221073	sw	80	399.30 $\pm$ .10	250438	da
30	*452.07 $\pm$ .03	221205	sw	81	396.77 $\pm$ .10	252035	-dw
31	451.98 $\pm$ .03	221249	sw	82	394.24 $\pm$ .07	253653	da
32	*451.86 $\pm$ .03	221307	sw	83	393.50 $\pm$ .07	254130	da
33	*451.69 $\pm$ .03	221391	sw	84	392.70 $\pm$ .07	254647	da
34	*451.56 $\pm$ .03	221455	sw	85	391.83 $\pm$ .05	255213	da
35	*451.45 $\pm$ .03	221508	sw	86	*391.44 $\pm$ .05	255467	sa
36	450.16 $\pm$ .03	222143	-sw	87	*390.49 $\pm$ .05	256088	da
37	449.93 $\pm$ .03	222257	+sw	88	390.04 $\pm$ .05	256384	sa
38	449.22 $\pm$ .03	222608	-sw	89	*389.48 $\pm$ .05	256753	da
39	448.29 $\pm$ .03	223070	+sw	90	*388.84 $\pm$ .05	257175	da
40	446.54 $\pm$ .05	223944	-sx	91	*388.37 $\pm$ .05	257486	sa
41	444.02 $\pm$ .03	225215	+sx	92	*388.05 $\pm$ .05	257699	sa
42	439.00 $\pm$ .2	227790	dw	93	*387.79 $\pm$ .05	257872	sa
43	434.30 $\pm$ .05	230256	-dw	94	*387.60 $\pm$ .05	257998	sa
44	433.98 $\pm$ .05	230425	sw	95	387.45 $\pm$ .05	258098	sa
45	427.15 $\pm$ .03	234110	sa	96	*387.08 $\pm$ .05	258345	-da
46	426.53 $\pm$ .05	234450	-da	97	386.26 $\pm$ .05	258893	-da
47	425.33 $\pm$ .07	235112	da	98	385.45 $\pm$ .07	259437	sa
48	424.05 $\pm$ .05	235821	dw	99	*385.03 $\pm$ .05	259720	-sw
49	423.61 $\pm$ .05	236066	sw	100	384.38 $\pm$ .05	260159	sa
50	423.17 $\pm$ .07	236312	dw	101	*384.03 $\pm$ .05	260396	-sw
51	422.58 $\pm$ .03	236642	sa	102	383.47 $\pm$ .05	260777	sa
				103	383.22 $\pm$ .05	260947	sa

TABLE 1. Code number, wavelength ( $\lambda$ ), wave number ( $\nu$ ), and profile type for all observed Kr resonances, listed in order of decreasing wavelength—Continued

Number	Wavelength ( $\text{\AA}$ )	Wave number ( $\text{cm}^{-1}$ )	Comment <sup>a</sup>	Number	Wavelength ( $\text{\AA}$ )	Wave number ( $\text{cm}^{-1}$ )	Comment <sup>a</sup>
104	382.95 $\pm$ .05	261131	sa	129	*367.03 $\pm$ .05	272457	+ sa
105	<sup>d</sup> 382.45 $\pm$ .05	261472	da	130	*366.70 $\pm$ .05	272702	+ sa
106	382.07 $\pm$ .05	261732	sa	131	*366.49 $\pm$ .05	272859	+ sa
107	381.87 $\pm$ .05	261869	sa	132	365.50 $\pm$ .2	273600	dda
108	381.51 $\pm$ .05	262116	sa	133	363.80 $\pm$ .2	274880	dda
109	381.31 $\pm$ .05	262254	sa	134	362.70 $\pm$ .2	275710	sa
110	380.80 $\pm$ .05	262605	sa	135	362.30 $\pm$ .2	276010	sa
111	379.30 $\pm$ .2	263640	dda	136	361.90 $\pm$ .2	276320	sa
112	*378.97 $\pm$ .05	263873	sa	137	359.60 $\pm$ .2	278090	sa
113	*378.65 $\pm$ .05	264096	sa	138	358.20 $\pm$ .2	279170	sa
114	*378.43 $\pm$ .05	264250	sa	139	357.30 $\pm$ .2	279880	sa
115	*378.23 $\pm$ .05	264389	sa	140	356.50 $\pm$ .2	280500	sa
116	375.03 $\pm$ .2	265390	dda	141	<sup>c</sup> 355.60 $\pm$ .2	281210	da
117	5.03 $\pm$ .05	266645	sa	142	354.80 $\pm$ .2	281850	da
118	374.66 $\pm$ .05	266909	sa	143	354.40 $\pm$ .2	282170	da
119	374.20 $\pm$ .05	267237	sa	144	350.30 $\pm$ .2	285470	da
120	373.00 $\pm$ .2	268100	dda	145	349.30 $\pm$ .2	286290	da
121	371.86 $\pm$ .05	268918	sa	146	348.30 $\pm$ .2	287110	da
122	371.37 $\pm$ .05	269273	sa	147	347.00 $\pm$ .2	288180	da
123	*370.87 $\pm$ .05	269636	sa	148	345.10 $\pm$ .2	289770	dda
124	*370.13 $\pm$ .05	270175	sw	149	343.50 $\pm$ .2	291120	da
125	*369.13 $\pm$ .05	270907	sa	150	342.30 $\pm$ .2	292140	sa
126	*368.60 $\pm$ .05	271297	sw	151	341.80 $\pm$ .2	292570	sa
127	*368.14 $\pm$ .05	271636	sa	152	341.10 $\pm$ .2	293170	sa
128	*367.56 $\pm$ .05	272064	+ sa	153	337.40 $\pm$ .3	296380	da

<sup>a</sup> Sign plus (+) or minus (−) represents the sign of  $q$  in the Fano [12] representation of noninteracting resonances. The letters s, d, dd, give a very rough idea of the sharpness or diffuseness of lines on a photographic plate. Naturally, this apparent width varies with gas pressure. The letters  $x$ ,  $w$  or  $a$  indicate specifically if the resonance has been measured at ( $x$ ) the point of highest rate of change of plate density, ( $w$ ) the point of maximum plate density, or ( $a$ ) the point of minimum plate density (maximum absorption); e.g.,  $sw$  means a sharp resonance of low unknown ( $q$ ) measured at the peak transmission point.

<sup>b</sup> Errors shown represent the estimated absolute uncertainty. In the case of Kr the relative accuracies are of the order of 0.02  $\text{\AA}$  better than the estimated absolute uncertainty.

<sup>c</sup> Resonances denoted by an asterisk (\*) are listed in table 3 as possible members of Rydberg series.

<sup>d</sup> Possible double resonance.

TABLE 2. Code number, wavelength ( $\lambda$ ), wave number ( $\nu$ ), and profile type for all observed Xe resonances, listed in order of decreasing wavelength

Number	Wavelength ( $\text{\AA}$ )	Wave number ( $\text{cm}^{-1}$ )	Comment <sup>a</sup>	Number	Wavelength ( $\text{\AA}$ )	Wave number ( $\text{cm}^{-1}$ )	Comment <sup>a</sup>
1	<sup>b</sup> 599.99 $\pm$ .05	166669	sw	17	556.51 $\pm$ .02	179691	+sx
2	595.93 $\pm$ .03	167805	−sw	18	555.52 $\pm$ .02	180012	−sw
3	<sup>c</sup> 591.77 $\pm$ .03	168985	+ dw	19	555.28 $\pm$ .02	180089	sw
4	589.54 $\pm$ .02	169624	−sw	20	552.31 $\pm$ .02	181058	+sx
5	586.29 $\pm$ .02	170564	−sw	21	552.00 $\pm$ .02	181159	sw
6	582.74 $\pm$ .02	171603	−sx	22	* 550.76 $\pm$ .02	181567	+sx
7	581.11 $\pm$ .02	172084	sw	23	549.60 $\pm$ .02	181951	sa
8	579.98 $\pm$ .02	172420	sw	24	549.19 $\pm$ .05	182086	sa
9	579.16 $\pm$ .02	172664	−sw	25	548.14 $\pm$ .02	182435	sa
10	570.79 $\pm$ .02	175196	sw	26	547.79 $\pm$ .02	182552	sa
11	570.47 $\pm$ .05	175294	sw	27	546.88 $\pm$ .02	182855	sa
12	562.39 $\pm$ .02	177813	sa	28	* 546.08 $\pm$ .02	183123	+sw
13	560.64 $\pm$ .05	178368	−sa	29	545.26 $\pm$ .02	183399	sw
14	560.44 $\pm$ .05	178431	+sa	30	544.95 $\pm$ .05	183503	sa
15	558.78 $\pm$ .02	178961	−sx	31	* 544.18 $\pm$ .02	183763	−sx
16	* 557.83 $\pm$ .02	179266	+sw	32	543.89 $\pm$ .02	183861	+sw

TABLE 2. Code number, wavelength ( $\lambda$ ), wave number ( $\nu$ ), and profile type for all observed Xe resonances listed in order of decreasing wavelength – Continued

Number	Wavelength( $\text{\AA}$ )	Wave number ( $\text{cm}^{-1}$ )	Comment <sup>a</sup>	Number	Wavelength( $\text{\AA}$ )	Wave number ( $\text{cm}^{-1}$ )	Comment <sup>a</sup>
33	543.49 $\pm$ .05	183996	<i>sw</i>	95	499.74 $\pm$ .03	200104	– <i>sw</i>
34	541.95 $\pm$ .02	184519	<i>sa</i>	96	498.54 $\pm$ .03	200586	<i>sa</i>
35	<sup>d</sup> 541.46 $\pm$ .05	184686	<i>sa</i>	97	497.33 $\pm$ .05	201074	<i>sw</i>
36	540.62 $\pm$ .02	184973	<i>sw</i>	98	497.06 $\pm$ .05	201183	+ <i>sx</i>
37	* 540.54 $\pm$ .02	185000	<i>sw</i>	99	496.11 $\pm$ .05	201568	<i>da</i>
38	* 539.33 $\pm$ .02	185415	– <i>sx</i>	100	495.69 $\pm$ .10	201739	<i>sa</i>
39	537.75 $\pm$ .02	185960	<i>sa</i>	101	495.42 $\pm$ .05	201849	<i>sw</i>
40	* 537.46 $\pm$ .02	186060	<i>sw</i>	102	495.15 $\pm$ .05	201959	<i>sw</i>
41	537.38 $\pm$ .02	186088	<i>sw</i>	103	495.02 $\pm$ .05	202012	<i>sa</i>
42	537.22 $\pm$ .02	186143	<i>sw</i>	104	494.39 $\pm$ .05	202269	– <i>sw</i>
43	536.83 $\pm$ .02	186279	– <i>sw</i>	105	493.80 $\pm$ .05	202511	– <i>sa</i>
44	535.95 $\pm$ .02	186585	– <i>sa</i>	106	493.42 $\pm$ .05	202667	– <i>sa</i>
45	* 535.55 $\pm$ .02	186724	<i>sw</i>	107	492.91 $\pm$ .03	202877	<i>sa</i>
46	535.13 $\pm$ .02	186870	– <i>sx</i>	108	492.10 $\pm$ .2	203210	<i>dda</i>
47	* 534.58 $\pm$ .02	187063	– <i>sx</i>	109	491.22 $\pm$ .03	203575	– <i>sw</i>
48	* 534.27 $\pm$ .02	187171	<i>sw</i>	110	490.20 $\pm$ .05	203998	– <i>sx</i>
49	<sup>d*</sup> 533.34 $\pm$ .05	187498	<i>sw</i>	111	489.93 $\pm$ .05	204111	<i>sa</i>
50	533.00 $\pm$ .02	187617	– <i>sw</i>	112	489.66 $\pm$ .03	204223	<i>sa</i>
51	* 532.76 $\pm$ .02	187702	<i>sw</i>	113	489.19 $\pm$ .03	204420	<i>da</i>
52	532.06 $\pm$ .02	187949	– <i>sw</i>	114	488.91 $\pm$ .03	204537	<i>sa</i>
53	531.83 $\pm$ .02	188030	– <i>sw</i>	115	488.59 $\pm$ .03	204671	+ <i>sa</i>
54	* 531.37 $\pm$ .02	188193	– <i>sw</i>	116	488.23 $\pm$ .03	204821	+ <i>sa</i>
55	* 531.21 $\pm$ .02	188249	<i>sw</i>	117	487.93 $\pm$ .03	204947	<i>sa</i>
56	531.04 $\pm$ .02	188310	<i>sw</i>	118	487.79 $\pm$ .03	205006	<i>sw</i>
57	* 530.93 $\pm$ .02	188349	<i>sw</i>	119	487.68 $\pm$ .03	205052	<i>sw</i>
58	* 530.83 $\pm$ .03	188384	<i>sw</i>	120	487.03 $\pm$ .05	205326	<i>sw</i>
59	* 530.74 $\pm$ .03	188416	<i>sw</i>	121	486.71 $\pm$ .05	205461	<i>sw</i>
60	530.10 $\pm$ .02	188644	– <i>sw</i>	122	485.55 $\pm$ .03	205952	+ <i>sw</i>
61	529.94 $\pm$ .03	188701	<i>sw</i>	123	485.25 $\pm$ .05	206079	– <i>sw</i>
62	* 529.34 $\pm$ .02	188914	<i>sw</i>	124	483.12 $\pm$ .05	206988	+ <i>sa</i>
63	528.93 $\pm$ .03	189061	<i>sa</i>	125	482.20 $\pm$ .05	207383	<i>sa</i>
64	* 528.42 $\pm$ .03	189243	+ <i>sa</i>	126	481.28 $\pm$ .05	207779	<i>sw</i>
65	* 528.05 $\pm$ .05	189376	+ <i>sw</i>	127	480.47 $\pm$ .05	208130	– <i>sa</i>
66	526.35 $\pm$ .02	189988	– <i>sw</i>	128	478.93 $\pm$ .10	208799	<i>da</i>
67	526.15 $\pm$ .02	190060	<i>sw</i>	129	478.30 $\pm$ .05	209074	<i>da</i>
68	525.86 $\pm$ .02	190165	<i>sw</i>	130	477.51 $\pm$ .05	209420	<i>da</i>
69	* 525.77 $\pm$ .02	190197	<i>sw</i>	131	477.12 $\pm$ .05	209591	<i>sw</i>
70	525.27 $\pm$ .03	190378	– <i>sw</i>	132	476.77 $\pm$ .05	209745	<i>sw</i>
71	521.97 $\pm$ .05	191582	<i>sw</i>	133	476.00 $\pm$ .3	210080	<i>dda</i>
72	521.81 $\pm$ .05	191641	<i>sw</i>	134	475.19 $\pm$ .05	210442	<i>sw</i>
73	521.54 $\pm$ .10	191740	<i>da</i>	135	* 474.36 $\pm$ .05	210810	<i>da</i>
74	518.88 $\pm$ .10	192723	<i>sa</i>	136	* 473.42 $\pm$ .05	211229	<i>da</i>
75	517.24 $\pm$ .10	193334	<i>da</i>	137	* 472.83 $\pm$ .05	211492	<i>sa</i>
76	514.42 $\pm$ .10	194394	<i>da</i>	138	* 472.36 $\pm$ .05	211703	<i>sa</i>
77	513.86 $\pm$ .10	194606	<i>da</i>	139	* 472.01 $\pm$ .05	211860	<i>sa</i>
78	513.27 $\pm$ .10	194829	<i>da</i>	140	* 471.67 $\pm$ .05	212013	<i>sa</i>
79	512.32 $\pm$ .05	195191	<i>sa</i>	141	* 470.46 $\pm$ .05	212558	<i>sa</i>
80	510.46 $\pm$ .05	195902	<i>sa</i>	142	* 469.40 $\pm$ .05	2130 <sub>0</sub>	<i>sa</i>
81	509.54 $\pm$ .03	196255	<i>sa</i>	143	* 468.67 $\pm$ .05	213370	<i>sa</i>
82	509.27 $\pm$ .03	196359	<i>sa</i>	144	* 468.15 $\pm$ .05	213607	<i>sa</i>
83	<sup>d</sup> 507.85 $\pm$ .10	196909	<i>dw</i>	145	467.72 $\pm$ .05	213803	<i>sa</i>
84	506.69 $\pm$ .05	197359	<i>sw</i>	146	467.54 $\pm$ .05	213885	<i>sa</i>
85	506.36 $\pm$ .05	197488	+ <i>sw</i>	147	467.02 $\pm$ .05	214124	<i>da</i>
86	505.89 $\pm$ .10	197671	<i>sa</i>	148	466.30 $\pm$ .2	214450	<i>da</i>
87	505.42 $\pm$ .03	197855	– <i>sx</i>	149	465.80 $\pm$ .05	214684	<i>sa</i>
88	504.40 $\pm$ .05	198255	– <i>sx</i>	150	465.10 $\pm$ .05	215008	<i>da</i>
89	503.64 $\pm$ .05	198555	– <i>sx</i>	151	464.35 $\pm$ .05	215355	<i>sa</i>
90	502.87 $\pm$ .05	198859	– <i>sx</i>	152	463.27 $\pm$ .07	215857	<i>sa</i>
91	502.13 $\pm$ .03	199152	– <i>sw</i>	153	462.63 $\pm$ .07	216155	<i>sa</i>
92	501.74 $\pm$ .05	199306	<i>sw</i>	154	462.23 $\pm$ .07	216343	<i>sa</i>
93	501.39 $\pm$ .05	199446	<i>sw</i>	155	* 461.00 $\pm$ .05	216920	+ <i>sa</i>
94	500.37 $\pm$ .05	199852	– <i>sw</i>	156	460.31 $\pm$ .10	217245	<i>dda</i>

TABLE 2. Code number, wavelength ( $\lambda$ ), wave number ( $\nu$ ), and profile type for all observed Xe resonances, listed in order of decreasing wavelength – Continued

Number	Wavelength( $\text{\AA}$ )	Wave number ( $\text{cm}^{-1}$ )	Comment <sup>a</sup>	Number	Wavelength( $\text{\AA}$ )	Wave number ( $\text{cm}^{-1}$ )	Comment <sup>a</sup>
157	*459.68 $\pm$ .05	217543	sa	206	*432.31 $\pm$ .05	231315	da
158	459.23 $\pm$ .05	217756	da	207	431.87 $\pm$ .05	231551	sa
159	*458.63 $\pm$ .05	218041	sa	208	*431.55 $\pm$ .05	231723	sa
160	*458.04 $\pm$ .05	218322	sa	209	*431.26 $\pm$ .05	231879	sa
161	456.80 $\pm$ .2	218910	da	210	*430.90 $\pm$ .05	232072	sa
162	456.71 $\pm$ .07	218957	–sa	211	*430.63 $\pm$ .05	232218	sa
163	456.42 $\pm$ .05	219096	–sa	212	*430.45 $\pm$ .05	232315	sa
164	455.83 $\pm$ .05	219380	sa	213	*430.31 $\pm$ .05	232391	sa
165	455.40 $\pm$ .05	219587	sa	214	429.67 $\pm$ .05	232737	+sa
166	454.95 $\pm$ .05	219804	–sa	215	428.36 $\pm$ .05	233448	sa
167	*454.34 $\pm$ .05	220099	–sa	216	428.14 $\pm$ .05	233568	sa
168	454.00 $\pm$ .05	220264	sa	217	427.92 $\pm$ .05	233689	sa
169	453.70 $\pm$ .05	220410	sa	218	426.61 $\pm$ .05	234406	+sa
170	*453.42 $\pm$ .05	220546	–sa	219	425.88 $\pm$ .05	234808	da
171	453.11 $\pm$ .07	220697	sa	220	425.51 $\pm$ .05	235012	da
172	452.70 $\pm$ .07	220897	–sx	221	424.97 $\pm$ .05	235311	sa
173	*452.35 $\pm$ .10	221068	dda	222	424.47 $\pm$ .10	235588	da
174	452.06 $\pm$ .07	221210	sa	223	424.02 $\pm$ .10	235838	da
175	450.33 $\pm$ .05	222059	–da	224	423.43 $\pm$ .10	236167	da
176	449.67 $\pm$ .05	222385	da	225	422.73 $\pm$ .10	236558	da
177	449.15 $\pm$ .05	222643	da	226	420.40 $\pm$ .2	237870	dda
178	448.42 $\pm$ .05	223005	da	227	418.00 $\pm$ .2	239230	dda
179	448.01 $\pm$ .05	223209	sa	228	413.70 $\pm$ .10	241721	da
180	447.61 $\pm$ .05	223409	da	229	410.30 $\pm$ .10	243724	da
181	445.91 $\pm$ .05	224260	sa	230	408.94 $\pm$ .10	244535	sa
182	*445.61 $\pm$ .05	224411	da	231	408.50 $\pm$ .10	244798	sa
183	445.41 $\pm$ .05	224512	da	232	407.67 $\pm$ .10	245296	sa
184	444.93 $\pm$ .05	224754	sa	233	406.32 $\pm$ .10	246111	sa
185	444.38 $\pm$ .05	225033	sa	234	406.07 $\pm$ .10	246263	sa
186	*443.73 $\pm$ .07	225362	da	235	404.96 $\pm$ .10	246938	sa
187	443.27 $\pm$ .05	225596	da	236	404.63 $\pm$ .10	247139	sa
188	442.91 $\pm$ .05	225779	da	237	403.87 $\pm$ .10	247604	sa
189	*442.41 $\pm$ .07	226035	da	238	401.90 $\pm$ .2	248820	da
190	*441.46 $\pm$ .10	226521	sa	239	401.24 $\pm$ .10	249227	sa
191	*441.01 $\pm$ .07	226752	sa	240	400.90 $\pm$ .10	249439	sa
192	*440.59 $\pm$ .07	226968	sa	241	399.94 $\pm$ .10	250038	da
193	*440.33 $\pm$ .07	227102	sa	242	399.56 $\pm$ .10	250275	da
194	439.92 $\pm$ .07	227314	da	243	399.00 $\pm$ .2	250630	da
195	439.30 $\pm$ .07	227635	da	244	397.72 $\pm$ .15	251433	da
196	438.29 $\pm$ .07	228159	sa	245	396.70 $\pm$ .2	252080	da
197	437.64 $\pm$ .07	228498	sa	246	395.66 $\pm$ .15	252742	da
198	437.22 $\pm$ .05	228718	sa	247	392.28 $\pm$ .15	254920	dda
199	436.82 $\pm$ .05	228927	sa	248	387.39 $\pm$ .15	258138	da
200	436.60 $\pm$ .05	229043	sa	249	385.62 $\pm$ .15	259323	da
201	436.15 $\pm$ .05	229279	+da	250	384.56 $\pm$ .15	260037	da
202	435.75 $\pm$ .05	229489	da	251	383.33 $\pm$ .15	260872	da
203	435.16 $\pm$ .05	229801	sa	252	377.20 $\pm$ .15	265111	da
204	*434.34 $\pm$ .05	230234	da	253	375.34 $\pm$ .15	266425	da
205	*433.30 $\pm$ .05	230787	da				

<sup>a</sup> Sign plus (+) or minus (–) represents the sign of  $q$  in the Fano [12] representation of noninteracting resonances. The letters  $s$ ,  $d$ ,  $dd$ , give a very rough idea of the sharpness or diffuseness of lines on a photographic plate. Naturally, this apparent width varies with gas pressure. The letters  $x$ ,  $w$ , or  $a$  indicate specifically if the resonance has been measured at ( $x$ ) the point of highest rate of change of plate density, ( $w$ ) the point of maximum plate density, or ( $a$ ) the point of minimum plate density (maximum absorption); e.g.,  $sw$  means a sharp resonance of low unknown ( $q$ ) measured at the peak transmission point.

<sup>b</sup> Errors shown represent the estimated absolute uncertainty. In the case of Xe the relative accuracies are of the order of 0.02  $\text{\AA}$  better than the estimated absolute uncertainty.

<sup>c</sup> Resonances denoted by an asterisk (\*) are listed in table 4 as possible members of Rydberg series.

<sup>d</sup> Possible double resonance.

The absorption cross section in the region of a resonance can be parameterized in the form:

$$\sigma(E) = \sigma_a \frac{(q + \epsilon)^2}{1 + \epsilon^2} + \sigma_b$$

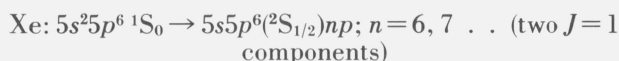
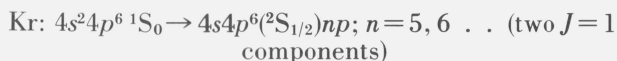
with  $\epsilon = (E - E_r)/\frac{1}{2}\Gamma$ , where the quantities  $E$  and  $E_r$  are the photon energy and the resonance energy ( $\epsilon = 0$ ), respectively. The parameter  $q$  is the resonance profile index and is defined in terms of transition matrix elements between the ground state, the modified discrete state and the continuum states. The half-width of the resonance is  $\Gamma$ , the quantity  $\sigma_a$  is the cross section associated with the fraction of the available continua with which the discrete state interacts, and  $\sigma_b$  is the cross section associated with the fraction of the continua which does not enter into the interaction. The parameter  $\rho$ , called the correlation index [12], is obtained from the relation  $\rho^2 = \frac{\sigma_a}{\sigma_a + \sigma_b}$ .

Experimentally, when  $q$  is positive, a region of low absorption at low energy immediately precedes a region of increased absorption at higher energy. For a negative  $q$ , the reverse is true. If  $q$  is of the order of 1, the resonance appears quite asymmetric. If  $q$  is large and  $\rho^2$  is small, the resonance looks like a conventional Lorentz absorption profile (absorption-type resonance), but if  $q$  is close to zero, the resonance has only a reduced-absorption zone (window-type resonance). When possible, in tables 1 and 2 the sign  $q$  is given. Where the letter  $x$ ,  $a$ , and  $w$  are used, the resonance appears to be an asymmetric, absorption or window-type resonance, respectively, and has been measured as such.

### 3.1. One-Electron Transitions

The most prominent series should be those associated with one-electron transitions. This was found to be the case in Ne and Ar, and is equally true in Kr and Xe. The ground state of the noble gases is a  $^1S_0$ . In a photoexcitation process, therefore, the upper state involved must have  $J=1$ , regardless of the coupling conditions.

Since strict  $L-S$  coupling is not applicable, the strongest Rydberg series would be due to transitions:



The upper configurations have *only* two  $J=1$  states, and transitions to upper states of other  $J$  cannot occur due to the rigorous selection rules:  $\Delta J=0, \pm 1$ ;  $0 \not\rightarrow 0$ .

Thus we might expect to resolve at low  $n$  values, the two  $J=1$  members converging to the known  ${}^2S_{1/2}$  limits of Kr II or Xe II. (This limit occurs in Kr at 450.62 Å and in Xe at 529.91 Å).

In the case of Kr, we see three "strong" window resonances in the region where the first members of the one-electron excitation series should occur. In Xe, one "strong" resonance and three somewhat weaker resonances are observed. "Strong" in this case means high visibility rather than a large oscillator strength, since the visibility of resonances depends also on the interference effects. Additionally, the ability to see window resonances is photographically enhanced at lower pressures.

The choice of the two  $J=1$  components of the first member of the Rydberg series is by no means unambiguous. The two components chosen in Kr are seen in the top photograph of figure 1 and again in the densitometer trace, figure 2. The resonances are denoted by their code numbers 3 and 5, see table 1. The wavelengths, principal quantum numbers ( $n$ ) and effective quantum numbers ( $n^*$ ) are given in table 3, part A. Recent work appears to support the above choice. Reader et al. [13] noted that the effective quantum number of the  $5p$  electron in the  $4s4p^65p$  state in the isoelectronic sequence Zr V, Nb VI, and Mo VII consistently differed from the  $n^*$  in the  $4s^2 4p^6 5p$  state of Nb V, Mo VI, and Tc VII by 0.040. Extrapolating this relationship the  $n^*$  for the  $4s4p^6 5p$  state of Kr I can be obtained from the  $n^*$  for the  $4s^2 4p^6 5p$  state of Rb I (2.289). The result, 2.329, is in good agreement with the value of 2.323 for the assigned resonance to this state in table 3.

In Xe, the most prominent member of the quartet of resonances (Code Nos. 1, 2, 3, 4) has been chosen as the first member of the one-electron excitation series: 3, 16, 28 etc. This series can be seen in the lower photograph of figure 1 and also in the densitometer trace figure 3. The wavelengths and effective quantum numbers are given in table 4, part A. A choice has not been made for the second  $J=1$  component in Xe, although it is likely to be resonance 1 or 2.

Recent work [13] suggests that the main  $J=1$  component in Xe should have an effective quantum number  $n^*=2.391$ . If resonance 4 is taken as the first member of the series, its effective quantum number is 2.398. Resonance 3 chosen here gives  $n^*=2.359$ . This choice was made upon the basis of the great similarity in resonance profiles of line 3 and the following members of the series, resonances 16 and 28. Figure 3 clearly shows that line 3 is asymmetric, with a low positive  $q$ , whereas resonance 4 has a  $q$  of the opposite sign. In fact, Ederer [10] has shown that the values of  $q$  and  $\rho^2$  for resonance 3 are  $0.23(\pm 0.04)$  and  $0.65(\pm 0.03)$ , for resonance 4 are  $-0.14(\pm 0.04)$  and  $0.50(\pm 0.04)$  and for resonance 16 are  $0.16(\pm 0.04)$  and  $0.67(\pm 0.02)$ . In addition, we can compare the equivalent one-electron excitation states in Ne, Ar, Kr, and Xe and the way in which the first member of the Rydberg series is always depressed (moved to longer wavelengths) relative to a simple theoretical estimate of its location, due to screening effects. The increase in this screening effect from Ne through Kr leads us to expect the strongest  $J=1$  component in Xe to lie almost exactly where it is. Nevertheless, it is conceivable that configuration interaction may cause resonances to interchange intensi-

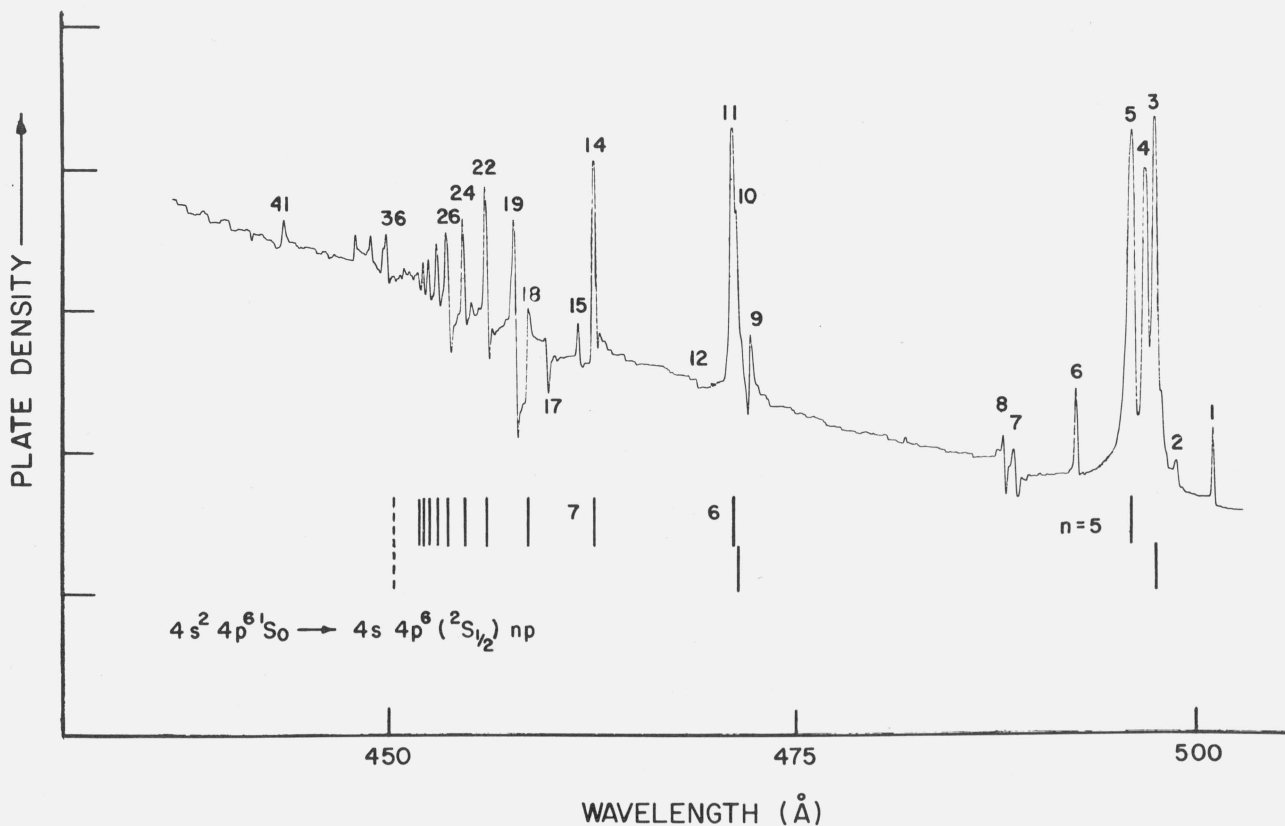


FIGURE 2. A microdensitometer trace of the absorption spectrum of Kr in the region 435-500 Å.

The main series of "window" resonances are indicated by vertical lines. Note the two  $J=1$  components for the  $n=5$  and 6 members. The code numbers alongside the resonances allow determination of their wavelengths (and in some cases classification) via tables 1 and 3.

TABLE 3. Resonances in Kr I grouped as members of possible series converging to the limits indicated

The principal quantum number ( $n$ ), and effective quantum number ( $n^*$ ) associated with the appropriate series limits are given. The levels in Kr II to which these series converge are arranged in order of increasing energy. Their positions are obtained from data [18] on the Kr II, added to 112915  $\text{cm}^{-1}$ , the first ionization energy of Kr I.

Code number	$\lambda$ (Å)	$n$	$n^*$	Code number	$\lambda$ (Å)	$n$	$n^*$
(A) Limit: $-4s4p^6(^2S_{1/2}) = 221915 \text{ cm}^{-1}$ ; Series: $-4s4p^6np$				(B) Unknown limit <sup>a</sup> = 240300 $\text{cm}^{-1}$			
5	496.07	5	2.323	63	417.96	13	10.26 <sup>a</sup> (9.35)
11	471.23	6	3.363	64	417.62	14	11.38 (10.18)
14	462.71	7	4.351	65	417.39	15	12.38 (10.88)
18	458.69	8	5.303	66	417.22	16	13.32 (11.49)
22	456.12	9	6.406	(C): $-4p^4(^1S)5s(^2D_{5/2}) = 258727 \text{ cm}^{-1}$ ; Series: $-4p^45snp$			
24	454.73	10	7.399	86	391.44	8	5.59
26	453.73	11	8.498	87	390.49	9	6.45
27	453.15	12	9.42	89	389.48	10	7.46
28	452.68	13	10.43	90	388.84	11	8.41
29	452.34	14	11.41	91	388.37	12	9.41
30	452.07	15	12.43	92	388.05	13	10.33
32	451.86	16	13.44	93	387.79	14	11.33
33	451.69	17	14.47	94	387.60	15	12.27
34	451.56	18	15.44	96	387.08	16	13.21
35	451.45	19	16.43	(D) Limit: $-4p^4(^1D)4d(^2D_{5/2}) = 262429 \text{ cm}^{-1}$ ; Series: $-4p^44dnp$			
Second series of two available, having $J=1$ final state				99	385.03	9	6.37
3	497.50	5	2.304	101	384.03	10	7.35
10	471.48	6	3.343				

TABLE 3. Resonances in Kr I grouped as members of possible series converging to the limits indicated—Continued

The principal quantum number ( $n$ ), and effective quantum number ( $n^*$ ) associated with the appropriate series limits are given. The levels in Kr II to which these series converge are arranged in order of increasing energy. Their positions are obtained from data [18] on the Kr II, added to 112915  $\text{cm}^{-1}$ , the first ionization energy of Kr I.

Code number	$\lambda$ (Å)	$n$	$n^*$	Code number	$\lambda$ (Å)	$n$	$n^*$
(E) Limit: $-4p^4(^1D)4d(^2P_{1/2}) = 265100 \text{ cm}^{-1}$ ; Series: $-4p^4dnp$							
112	378.97	12	9.46	127	368.14	10	7.27
113	378.65	13	16.46	128	367.56	11	8.17
114	378.43	14	11.36	129	367.03	12	9.36
115	378.23	15	12.43	130	366.70	13	10.44
				131	366.49	14	11.35
(F) Limit <sup>b</sup> : $-4p^4(^1D)4d(^2S_{1/2}) = 273710 \text{ cm}^{-1}$ ; Series: $-4p^4dnp$				(G) Limit: $-4p^4(^1S)4d(^2D_{5/2}) = 273927 \text{ cm}^{-1}$ ; Series: $-4p^4dnp$			
123	370.87	8	5.19	124	370.13	8	5.41
125	369.13	9	6.26	126	368.60	9	6.46

<sup>a</sup> The nearest known limit [18] is  $(^1D)5s(^2D_{3/2})$  at 240512  $\text{cm}^{-1}$ . One could assume this limit to be the appropriate one, giving the values of  $n^*$  shown in parentheses. Noninteger difference in  $n^*$  through the series could possibly be explained by configuration interaction effects.

<sup>b</sup> This limit was previously assigned [19] to  $4p^4(^3P)5d(^1P_{1/2})$ . It was recently reassigned [18] by Minnhagen.

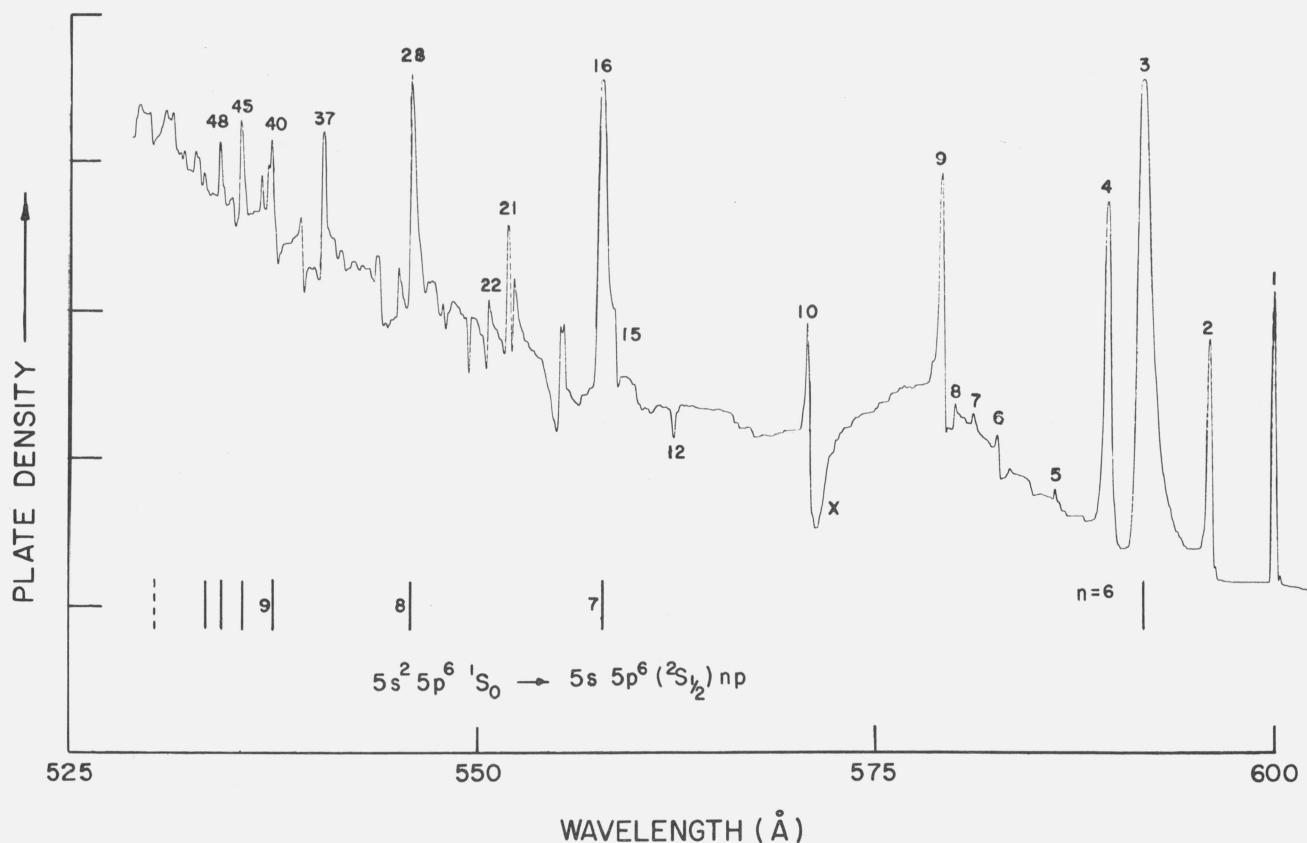


FIGURE 3. A microdensitometer trace of the absorption spectrum of Xe in the region 525–600 Å.

The main series of “window” resonances is denoted by vertical lines. The code numbers allow determination of wavelengths (and in some cases classification) via tables 2 and 4. The absorption feature labeled X, is the third order of an absorption line [4] at 190.41 Å.

TABLE 4. Resonances in Xe I grouped as members of possible series converging to the limits indicated

The principal quantum number ( $n$ ) and effective quantum number ( $n^*$ ) associated with the appropriate series limits are given. The levels in Xe II to which these series converge are obtained by adding 97834 cm<sup>-1</sup>, the lowest ionization energy of Xe I, to terms [19] of Xe II.

Code number	$\lambda$ (Å)	$n$	$n^*$	Code number	$\lambda$ (Å)	$n$	$n^*$
(A) Limit: $-5s5p^6(^2S_{1/2})=188708$ cm <sup>-1</sup> ; Series: $-5s5p^6np$				(E) Limit: $-5p^4(^3P)6p(^4D_{3/2})=214617$ cm <sup>-1</sup> ; Series: $-5p^46pnd$ <sup>d</sup>			
3	591.77	6	2.359	141	470.46	10	7.30
16	557.83	7	3.409	142	469.40	11	8.34
28	546.08	8	4.433	143	468.67	12	9.38
<sup>a</sup> 37	540.54	9	5.440	144	468.15	13	10.42
40	537.46	10	6.438	(F) Limit: $-5p^4(^3P)6p(^4S_{3/2})=219463$ cm <sup>-1</sup> ; Series: $-5p^46pnd$			
45	535.55	11	7.437	155	461.00	9	6.57
48	534.27	12	8.450	157	459.68	10	7.56
<sup>b</sup> 49	533.34	13	9.52	159	458.63	11	8.78
51	532.76	14	10.44	160	458.04	12	9.80
55	531.21	19	15.47	(G) Limit: $-5p^4(^1S)5d(^2D_{3/2})=222136$ cm <sup>-1</sup> ; Series: $-5p^45dnp$			
57	530.93	21	17.48	167	454.34	11	7.34
58	530.83	22	18.41	170	453.42	12	8.31
59	530.74	23	19.39	173	452.35	13	9.41
(B) Limit: $-5p^4(^3P)6s(^4P_{3/2})=190902$ cm <sup>-1</sup> ; Series: $-5p^46snp$				(H) Limit: $-5p^4(^1D)6p(^2F_{7/2})=227898$ cm <sup>-1</sup> ; Series: $-5p^46pnd$			
22	550.76	7	3.429	182	445.61	8	5.61
38	539.33	8	4.472	186	443.73	9	6.58
47	534.58	9	5.346	189	442.41	10	7.67
54	531.37	10	6.364	190	441.46	11	8.93
62	529.34	11	7.431	191	441.01	12	9.79
65	528.05	12	8.480	192	440.59	13	10.87
(C) Limit: $-5p^4(^3P)6s(^4P_{3/2})=192898$ cm <sup>-1</sup> ; Series: $-5p^46snp$				193	440.33	14	11.74
31	544.18	7	3.466	(I) Limit: $-5p^4(^3P)7s(^4P_{1/2})=232895$ cm <sup>-1</sup> ; Series: $-5p^47snp$			
<sup>b</sup> 49	533.34	8	4.508	204	434.34	10	6.42
64	528.42	9	5.480	205	433.30	11	7.22
69	525.77	10	6.374	206	432.31	12	8.34
(D) Unknown Limit <sup>c</sup> =212665 cm <sup>-1</sup>				208	431.55	13	9.68
135	474.36	8	7.691	209	431.26	14	10.39
136	473.42	9	8.742	210	430.90	15	11.55
137	472.83	10	9.68	211	430.63	16	12.73
138	472.36	11	10.68	212	430.45	17	13.76
139	472.01	12	11.68	213	430.31	18	14.75
140	471.67	13	12.97				

<sup>a</sup> The resonance at 540.62 Å is an alternative choice for the  $n=9$  member.

<sup>b</sup> This resonance appears to be double and is used in series (A) and (C).

<sup>c</sup> The nearest Xe II levels are  $5p^4(^1D)5d(^2F_{5/2, 7/2})$  at 212585 cm<sup>-1</sup> and 212748 cm<sup>-1</sup>, either of which would allow an  $nf$  series.

<sup>d</sup> The quantum defects for this series are more appropriate to a running  $p$  electron. However, assuming a correct assignment for the level in Xe II, parity considerations require a running  $d$  electron (or an  $s$  electron).

ties, and affect their shapes. Good theoretical calculations will be required to resolve this situation.

If we move to higher series members in Kr, we find that resonance 18 has an unusually low effective quantum number and a low intensity (see fig. 2). On the basis of the quantum defect alone, resonance 18, the  $n=8$  member of this series, was chosen as a member of the Rydberg series. Clearly, resonance 19 is much “stronger” (see also Ederer [10]) and was observed by Samson [15] and classified as a member

of the series with  $n^*=5.593$ . Once again, there is ambiguity. The remainder of the series is quite definitely established on a basis of quantum defects, intensities and profiles.

In tracing the development of the Xe series, we find the  $n=9$  member to be double and an arbitrary choice must be made from resonances 36 and 37. Other workers [14, 15] did not resolve these resonances. Configuration interactions cause members  $n=15$  through 18 and  $n=20$  to be missing.

TABLE 5. *A comparison of the wavelengths of some of the resonances measured in the present work and those of other workers*

The Siegbahn [16] wavelengths are obtained using the conversion factor  $\lambda = 12398/E(\text{eV})$ .

Krypton				Xenon				
Code	Present work	Samson [15]	Siegbahn [16]	Code	Present work	Samson [15]	Mansfield [17]	Siegbahn [16]
1	501.23	501.14		1	599.99	599.95	599.81	
3	497.50	497.44	497.1	2	595.93	595.92	595.83	
4	496.90	496.85		3	591.77	591.81	591.67	592.1
5	496.07	496.00	495.7	4	589.54	589.62	589.50	589.5
10	471.48	471.55	471.2	5	586.29		586.24	
14	462.71	462.69	462.8	6	582.74		582.72	
18	458.69		458.8	7	581.11		581.07	
19	<sup>a</sup> 457.86	457.85		8	579.98		579.94	
22	456.12	456.10	456.0	9	579.16	<sup>14</sup> 579.25	579.15	
24	454.73	454.71	455.0	10	570.79	<sup>14</sup> 570.90	570.80	
26	453.73	453.71	453.8	15	558.78		558.78	
27	453.14	453.14		16	557.83	557.92	557.86	557.7
29	452.32	452.32		19	555.28		555.32	
30	452.07	452.01		21	552.00	<sup>14</sup> 552.07	552.02	
32	451.86	451.85		22	550.76		550.77	
				28	546.08	546.16		546.2
				<sup>b</sup> 36	540.62			540.5
				37	540.54	540.71		
				40	537.46	537.40		
				45	535.55	535.62		

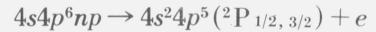
<sup>a</sup> Resonance 18 was chosen in the present work, on the basis of quantum defect; for  $4s4p^68p$ . However, resonance 19 is a considerably stronger line seen also by Samson and assigned to the  $8p$  state.

<sup>b</sup> Two resonances, equally strong, just resolved.

Finally, in table 5, we see a comparison of the long wavelength resonances in Kr and Xe with other workers. In Kr, the present data is compared with the photoabsorption work of Samson [14, 15] and the electron spectroscopic observations of Siegbahn and co-workers [16]. In Xe, comparison is also made with the photoabsorption work of Mansfield [17] (Mansfield measured Kr also, and was in agreement with the present work for the stronger transitions). The error limits quoted by Samson are  $\pm 0.05 \text{ \AA}$ , those of Siegbahn et al. are of the order of  $0.2 \text{ \AA}$ . Mansfield gave no estimated error, but he had some calibration problems in the region of  $585\text{--}600 \text{ \AA}$  due to lack of standards. The accuracy of the present measurements is also impaired in this region of the spectrum because of slight instrumental errors and this is reflected in the somewhat increased error limits given to the resonances in that region. Almost all of the wavelengths of Samson agree, within the combined error limits, with the present data, even in the range  $585\text{--}600 \text{ \AA}$ .

The data of Siegbahn et al. was obtained by firing electrons of an energy of several keV into the noble gases, and measuring the energies (typically 8 to 14 eV) of the electrons released in the subsequent autoionization process, with a spherical electrostatic analyzer. Rydberg series of electron lines were found corresponding to transitions from excited states of neutral atoms to the ground state of the ions. By measuring the

kinetic energy of electrons produced in the autoionization process:



and knowing the energy of the  $4s^24p^5(^2P_{1/2, 3/2})$  states of Kr II, they were able to calculate the energy of the excited state before autoionization. Since the Siegbahn data was normalized to the present data at certain wavelengths, it cannot be thought of as independent. It is interesting, however, to note that these workers picked out a second  $J=1$  component for the  $4s4p^65p$  state of Kr. Even though the absolute wavelengths of resonances 3 and 5 disagree by  $0.3 \text{ \AA}$ , the difference in wavelengths of  $1.4 \text{ \AA}$  is in agreement with the present data. In Xe, however, the implication might be that resonances 3 and 4 are the two  $J=1$  components, in agreement with another recent estimate [13], and in disagreement with the present classification. It should be pointed out, however, that excitation by electron bombardment can excite, in general, many transitions not allowed optically and that often such nonoptically allowed transitions are preferred. In addition, the resonance profiles may be completely different.

### 3.2. Two-Electron Transitions

It has been pointed out that only two  $J=1$  components can be expected for states such as  $4s4p^65p$  in Kr.

The remaining resonances in Kr, such as 1, 2, 4, 6, 7, 8 etc. (see fig. 2) must therefore be classified, from energy considerations, in terms of *two*-electron transitions, viz:



Here  $ll' = sp, sf, pd, pf$ .

The term possibilities are just those outlined previously in Ar [3]. As shown, the grandparent term may be  ${}^3\text{P}$ ,  ${}^1\text{D}$ , or  ${}^1\text{S}$ . Taking the simplest case of  $5s5p$  in Kr, the number of possible  $J=1$  components is 14, with 3 of these being  ${}^1\text{P}_1$ , in strict  $L-S$  coupling. We know, however, that  $L-S$  coupling does not prevail, and we may expect a large number of excited states with  $J=1$ . Experimentally, one observes few of this potentially large number of resonances.

As in Ar, we can make crude estimates of the expected positions of resonances from the known levels of the ion [18, 19] and typical quantum defects for the  $s$ ,  $p$ ,  $d$ , and  $f$  electrons. Because the spectra observed are quite rich and because of screening and configuration interaction effects, such estimates cannot be sufficiently accurate to establish definite assignments.

In the cases of Ne and Ar a number of low-lying two-electron excitation states were identified. In Kr and Xe virtually none have been assigned. In the absence of good calculations, we can only identify series with high-lying members. Intensity sharing interactions appear to be responsible for the fact that we see any series at all.

In both Kr and Xe, quantum defects have been calculated for all the resonances to the available [18, 19] known limits. As a result of this analysis, only 28 resonances in Kr and 43 in Xe have been grouped into probable Rydberg series. In the Ar case, one experimental fact was very obvious—that of all the possible excited configurations, those of the type:— $3p^4 3dnl$  and  $3p^4 4snl$  dominated the spectrum. Series such as  $3p^4 4pns$  were hardly in evidence. This tendency is equally pronounced in Kr, where *all* of the series are of the type  $4p^4 5snp$  or  $4p^4 4dnp$ .

Turning to table 3 (B), the unidentified series having a limit at  $240300 \text{ cm}^{-1}$  may be due to transitions to states  $({}^1\text{D})5s({}^2\text{D}_{3/2})np$ . However, using Minnhagen's value for this limit [18], we must then invoke certain configuration interaction effects to explain the unusual run of effective quantum numbers (inside the brackets).

In Xe, if the present tentative assignments are correct, the emphasis on running electrons of odd parity is no longer evident. Indeed, there are apparently two series of the type  $5p^4 6pnd$ . Another series is tentatively labelled  $6pnd$  (table 4 (E)) but the defects are more appropriate for a running  $p$  electron—*forbidden* on the grounds of nonconservation of parity *if* the state in Xe II has been correctly identified [19].

Also in table 4, the series (D) with an unidentified limit, may well be associated with a series of the type  $5p^4 5dnf$ .

Some of the more obvious series in Kr and Xe are indicated by lines above and below the spectra of figure 1. In Kr we can see the series A, B, C, F and G of table 3; in Xe we see the series A, B, D and I of table 4.

## 4. Conclusions

The one- and two-electron excitation resonances listed into the series above represent only one quarter of those observed. The basic problem is one of unfolding the complicated configuration interactions present, which displace levels from the locations expected on simple theoretical grounds, and produce intensity anomalies. Even within a single series, the profiles of the resonances may change with increasing principal quantum number. In others, only high series members are evident. It appears that a substantial theoretical effort will be required to analyze the spectra further, even in those regions where relatively few resonances occur. Original prints of the spectra shown in figure 1 can be made available to those interested in furthering the interpretation.

## 5. References

- [1] Madden, R. P., and Codling, K., *Astrophys. J.* **141**, 364 (1965).
- [2] Codling, K., Madden, R. P., and Ederer, D. L., *Phys. Rev.* **155**, 26 (1967).
- [3] Madden, R. P., Ederer, D. L., and Codling, K., *Phys. Rev.* **177**, 136 (1969).
- [4] Codling, K., and Madden, R. P., *Phys. Rev. Letters* **12**, 106 (1964).
- [5] Codling, K., and Madden, R. P., *Appl. Opt.* **4**, 1431 (1965).
- [6] Beutler, H., *Zeit. Phys.* **93**, 177 (1935).
- [7] Samson, J. A. R., *Phys. Rev.* **132**, 2122 (1963).
- [8] Madden, R. P., and Codling, K., *J. Opt. Soc. Am.* **54**, 268 (1964).
- [9] Codling, K., and Madden, R. P., *Phys. Rev.* **A4**, 2261, (1971).
- [10] Ederer, D. L., *Phys. Rev.* **A4**, 2263, (1971).
- [11] Madden, R. P., Ederer, D. L., and Codling, K., *Appl. Opt.* **6**, 31 (1967).
- [12] Fano, U., and Cooper, J. W., *Phys. Rev.* **137**, A1364 (1965).
- [13] Reader, J., Epstein, G. L., and Ekberg, J. O., *J. Opt. Soc. Am.* (in press).
- [14] Samson, J. A. R., *Phys. Letters* **8**, 107 (1964).
- [15] Samson, J. A. R., *Advances in Atomic and Molecular Physics* (Academic Press Inc. New York 1966) Vol. 2, p. 177.
- [16] Siegbahn, K., Nordling, C., Johansson, C., Hedman, J., Heden, P. F., Hamrin, K., Gelius, U., Bergmark, T., Werme, L. O., Manne, R., and Baer, Y., *ESCA Applied to Free Molecules* (North-Holland Publishing Co., Amsterdam 1969).
- [17] Mansfield, M. W. D., Ph.D. Thesis, Physics Dept., Imperial College London (1969).
- [18] Minnhagen, L., Strihed, H., and Peterson, R., *Arkiv. för Fys.* Bd 39 nr **34**, 471 (1969).
- [19] Moore, C. E., *Atomic Energy Levels*, Nat. Bur. Stand. (U.S.) Circ. 467, Vols. **2** and **3** (1952, 1958).

(Paper 76A1-693)